Re-examination of the room temperature crystal structure of $CuGeO_3$ by x-ray diffraction experiments: observation of new superlattice reflections

1997 J. Phys.: Condens. Matter 9 809

(http://iopscience.iop.org/0953-8984/9/4/003)

J. Phys.: Condens. Matter **9** (1997) 809–824. Printed in the UK PII: S0953-8984(97)78977-X

Re-examination of the room temperature crystal structure of $CuGeO_3$ by x-ray diffraction experiments: observation of new superlattice reflections

M Hidaka†, M Hatae†, I Yamada‡¶, M Nishi§ and J Akimitsu‖

† Department of Physics, Faculty of Science, Kyushu University, Hakozaki, Higashi-ku, Fukuoka 812, Japan

‡ Department of Physics, Faculty of Science, Chiba University, Yayoi-cho, Inage-ku, Chiba 263, Japan

§ The Institute for Solid State Physics, The University of Tokyo, Roppongi, Minato-ku, Tokyo 106, Japan

‖ Department of Physics, Aoyama-Gakuin University, 6-16-1 Chitosedai, Setagaya-ku, Tokyo 157, Japan

Received 28 October 1996

Abstract. A recent electron paramagnetic resonance (EPR) study of $CuGeO_3$ revealed the existence of an antisymmetric exchange interaction, $\sum_i \boldsymbol{d}_{ii+1} \cdot (\boldsymbol{S}_i \times \boldsymbol{S}_{i+1})$, between Cu spins on the *c*-axis in this compound (Yamada I, Nishi M and Akimitsu J 1996 *J. Phys.: Condens. Matter* **8** 2625). To allow this interaction, the crystal structure must have no inversion centre halfway between relevant Cu sites. However, the structure with the space group *Pbmm* (D_{2h}^5), which was proposed for this compound by Völlenkle *et al* and has been accepted so far, does not allow this interaction because it has an inversion centre at the midpoint between nearest-neighbour Cu sites on the *c*-axis. This conflict was pointed out in the EPR study and was taken to indicate the inconsistency of the structure with *Pbmm*. To find the correct crystal structure of $CuGeO_3$, x-ray diffraction experiments are performed at room temperature on samples which are markedly improved in their quality because they are produced by the annealing and slow cooling of single crystals grown by the floating-zone method. As a result, new superlattice reflections which had not been reported so far are detected. The space group and the unit cell are determined to be $P2_12_12$ (D_2^3) and $2a_p \times b_p \times 4c_p$, respectively, where $a_p \times b_p \times c_p$ is the pseudo-unit cell proposed by Völlenkle *et al*. The newly found structure allows the antisymmetric interaction mentioned above. Possible connections between the new structure and the question of why the structural transition, which brings about the dimerization of Cu spins, occurs in $CuGeO_3$ are discussed.

1. Introduction

Since the report by Hase *et al* [1] in which the spin–Peierls transition in the inorganic compound $CuGeO_3$ was first strongly suggested, various investigations have been made of this compound and their results have also supported the assertion that a transition occurs. For example, neutron [2, 3], x-ray [3] as well as electron diffraction [4] experiments found a structural transition which accompanied the dimerization of Cu ions along the *c*-axis, while an inelastic neutron scattering study [5] confirmed the spin–Peierls energy gap.

¶ To whom any correspondence should be addressed; e-mail: yamada@science.s.chiba-u.ac.jp.

0953-8984/97/040809+16$19.50

The room temperature crystal structure of this compound was first reported by Völlenkle *et al* [6] about three decades ago. They proposed, on the basis of their x-ray diffraction experiments, that the lattice parameters at room temperature are $a_p = 4.81$ Å, $b_p = 8.47$ Å and $c_p = 2.94$ Å, and the space group is *Pbmm* (D_{2h}^5); the subscript p attached to a, b and c means that these three parameters are pseudo-parameters, as will be clarified later in the present report. According to their report, the structure consists of CuO_6 octahedra and GeO_4 tetrahedra, both of which are slightly distorted from their respective regular shapes, and are individually stacked along the c-axes. The distorted shapes of the CuO_6 (GeO_4) are identical to one another. The adjacent CuO_6 octahedra aligned along the c-axis share two O ions with each other and are arranged quasi-one-dimensionally, while the GeO_4 tetrahedra are also chained with one of their edges constrained to be parallel to the c-axis. Each O ion is shared with these two kinds of polyhedron. The respective principal axes of the stacked CuO_6 octahedra are parallel to one another, and the same applies to the stacked GeO_4 tetrahedra.

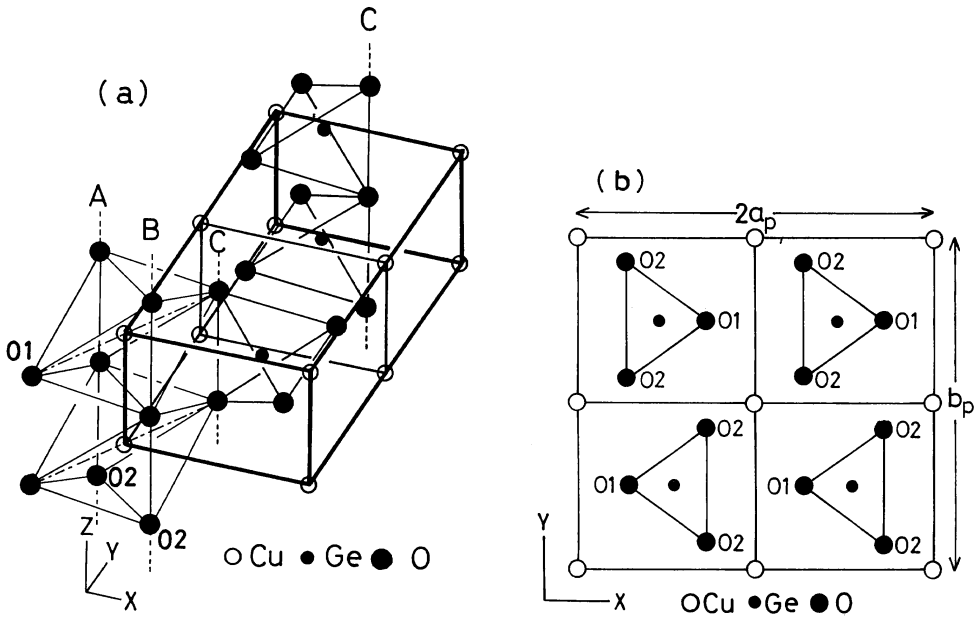

Figure 1. An outline of the structure reported by Völlenkle *et al*. (a) The pseudo-unit cell, $a_p \times b_p \times c_p$, is shown by bold lines. The CuO_6 octahedra and GeO_4 tetrahedra are stacked along the Z-direction, where the coordinate system $[X\ Y\ Z]$ is taken as $\boldsymbol{X} \| \boldsymbol{a}_p$, $\boldsymbol{Y} \| \boldsymbol{b}_p$ and $\boldsymbol{Z} \| \boldsymbol{c}_p$. The straight lines A and B indicate quasi-one-dimensional stacking of the CuO_6 octahedra, while the other straight line C is formed as a result of one-dimensional linkage of one of the edges of the GeO_4 tetrahedra. The O ions denoted as 01 and 02 correspond to O_1 and O_2 given in [6], respectively. (b) The Z-projection of the cell $2a_p \times b_p \times c_p$.

Figure 1 shows an outline of the structure reported in [6]. Figure 1(a) schematically shows the arrangement of ions in the pseudo-unit cell $a_p \times b_p \times c_p$, which is indicated by bold lines; the quasi-one-dimensional stacking of the CuO_6 octahedra is indicated by the two lines A and B, while the line formed by the linkage of one of the edges of the GeO_4 tetrahedra is indicated as C. The coordinates $[X\ Y\ Z]$ are taken to be parallel to the crystal axes $[a\ b\ c]$, respectively. The three lines, A, B and C, are parallel to the c-axis. The cell

$2a_p \times b_p \times c_p$ projected on the Z-plane is shown in figure 1(b), in which we see that the O ions have two kinds of site, denoted as 01 and 02, and each CuO_6 octahedron is surrounded by four GeO_4 tetrahedra.

Although the crystal structure of the present compound reported in [6] was re-examined over a couple of years by diffraction experiments including those of [2–4] and by other methods, no symmetries which were not encompassed by *Pbmm* were reported until recently. However, a recent electron paramagnetic resonance (EPR) investigation [7] came to the conclusion that the crystal symmetry of this compound should be lower than that with the space group *Pbmm* on the basis of the following fact: the EPR study confirmed the existence of the Dzyaloshinsky–Moriya (DM) antisymmetric exchange interaction, $\sum_i \boldsymbol{d}_{ii+1} \cdot (\boldsymbol{S}_i \times \boldsymbol{S}_{i+1})$ with $\boldsymbol{d}_{ii+1} \perp c$-axis, between nearest-neighbour Cu spins on the c-axis. As is well established, a DM interaction is allowed only when the crystal symmetry has no inversion centre at the midpoint between the relevant magnetic ions [8], but the symmetry with *Pbmm* as space group has an inversion centre at the midpoint of the nearest-neighbour Cu sites on the c-axis.

On the basis of these facts, the inappropriateness of the crystal symmetry with space group *Pbmm* was strongly suggested in the EPR study [7]. Since the local symmetry around relevant Cu ions is concerned in the DM interaction, we guess, on the basis of the EPR experiments referred to above, that the nearest-neighbour CuO_6 octahedra which share two O ions with each other along the c-axis are distorted in different ways from each other for some reason. If such differently distorted octahedra are periodically stacked along the c-axis, a superlattice structure will be formed which should yield reflections in the diffraction patterns obtained by x-ray, neutron and electron diffraction experiments. However, no observations of such reflections have been reported so far, although several diffraction experiments have been performed on this compound. The contradiction between the EPR result and the crystal symmetry with space group *Pbmm* led us to doubt the quality of the single crystals used so far in the diffraction experiments performed on this compound. The meaning of the word 'quality' used in this report will become clear in the following paragraphs.

As reported in [6], the samples employed by Völlenkle *et al* were prepared by sintering a mixture of CuO and GeO_2 at 1000 °C. We doubt the quality of their samples because it is almost impossible to get high-quality crystals by just sintering the raw materials. In most of the experiments performed in the past few years to examine the spin–Peierls transition, use was made of as-grown single crystals obtained by the floating-zone (FZ) method employing an image furnace. This method has several advantages, but also has a disadvantage as regards growing single crystals of a compound which consists of several kinds of ion, like the present compound. Since light power is focused in a narrow band on a raw material formed into a rod, the temperature gradient induced along the travelling axis is extremely steep. Thus there is the possibility that crystallization finishes before the atoms, which are loosely connected with their neighbouring atoms, have occupied proper stable sites, and then the atoms randomly occupy virtual sites as if the sample had simply been quenched.

Let us take $CuGeO_3$ as an example. Since the interionic potentials of Cu–O and Ge–O are stronger than those of O–O, the CuO_6 octahedra and the GeO_4 tetrahedra will be formed in an early stage of crystallization. In the next stage, these two kinds of polyhedron, which share O ions with each other, will be stacked individually along the c-axes and finally this compound will complete the crystallization accompanying the respective distortions of the CuO_6 octahedra and the GeO_4 tetrahedra to reduce the total interionic potential energies.

We can now explain how the symmetry with space group *Pbmm* does not necessarily indicate the structure of $CuGeO_3$ as proposed in [6]. Let us suppose that the intrinsic crystal structure of $CuGeO_3$ involves CuO_6 octahedra (GeO_4 tetrahedra) which are distorted in

several different ways from one another, and are periodically stacked along the *c*-axis in their respective patterns of distortion. In such crystals, an order of distortions is created. When the coherence length of the order is long enough for the respective diffraction techniques to be used, the order can yield additional superlattice reflections. On the other hand, no order of the distortions is created when the differently distorted CuO_6 octahedra (GeO_4 tetrahedra) are stacked without any periodicity or regularity of the distortions, i.e., there is a complete absence of coherency of the distortions, and therefore no superlattice reflections are expected from such a crystal. Consequently, experimental results which lack the superlattice reflections coming from such an order of distortions do not necessarily indicate the absence of the structure which accompanies differently distorted CuO_6 octahedra (GeO_4 tetrahedra). That is why we doubt the conclusion given in [6]. We think that the crystal structure reported in [6] merely reflects an average of several differently distorted CuO_6 octahedra (GeO_4 tetrahedra).

Since the difference between the total interionic potential energies of the ordered and disordered states of the distortions is expected to be small, the order of the distortions is easily destroyed at high temperatures by the thermal fluctuations of the lattice. Whether a crystal of $CuGeO_3$ has the coherency mentioned above or not depends on how the melt is cooled down. What about as-grown crystals of $CuGeO_3$ obtained by the FZ method? As explained earlier in this section, crystallization in this method finishes too quickly due to the steep temperature gradient. Accordingly, it is possible that the O ions are frozen at virtual sites, a fact which destroys the regularity of the stacking of the differently distorted CuO_6 octahedra (GeO_4 tetrahedra) along the *c*-axis. It is thus extremely hard for the crystals to maintain the coherency of the distortions of the CuO_6 octahedra and GeO_4 tetrahedra. As long as one uses as-grown crystals obtained by fast cooling, as in the FZ method, it is probably impossible to clarify the crystal structure of the present compound more accurately than was reported in [6].

For this reason, we reached the conclusion that as-grown single crystals of $CuGeO_3$ obtained by the FZ method must be improved in quality to answer the questions raised by the EPR experiments [7]. Now the meaning of the word ‘quality’ used in the present report becomes clear. That is, the quality of the samples depends on whether they have coherent distortions or not. Annealing and slow cooling of the as-grown crystals constitute a simple method of improving the quality of single crystals grown by the FZ method. As will be shown later, we found that such a treatment was very effective for improving the quality of $CuGeO_3$ single crystals. Using the carefully treated samples, we found new superlattice reflections which were absent in the reports given by Völlenkle *et al* and by others. On the basis of the present experimental results, we determine the space group and the unit cell, respectively, and show that the newly determined structure allows the DM interaction. Moreover, we point out that the newly found superlattice structure along the *c*-axis is very unstable, and, as a result, lattice instability is induced with the change of temperature, which should be closely related to the reason for the structural transition accompanying the dimerization of Cu spins occurring in the present inorganic compound. There are several unsolved problems concerning the spin–Peierls transition of the present compound. We suggest that those problems are closely related to the quality of the samples used.

2. Experimental details

As explained in section 1, improving the quality of the single crystals obtained by the FZ method is a key point as regards obtaining a fruitful result in the present study. Using the FZ method, we first grew a rod-type single crystal of the present compound. It was cut into

small pieces the sizes of which were suited to the respective x-ray diffraction experiments employed in the present study, and these were then annealed in an O_2 gas atmosphere for several hours at 1150 °C, which is slightly lower than the melting temperature, and were cooled at 2 °C h^{-1}. (Our differential thermal analysis yielded the melting temperature as 1176 ± 5 °C.) We strictly controlled the temperature of the furnace while the samples were cooled down; otherwise the slow cooling would have provided no benefit. Such treatment of samples, which were prepared by cleaving or cutting the as-grown crystals, also enabled us to sweep away unexpected distortions or strains produced during the cutting or cleaving of the crystal. We found that the samples thus treated exhibited distinct reflections, including new ones which were impossible to detect in the sample prepared from the as-grown crystal.

Using a Weissenberg camera as well as a four-circle x-ray diffractometer, we performed experiments at room temperature. To detect very weak reflections more accurately, we also employed an energy-dispersive x-ray diffraction method.

3. Experimental results

3.1. Preliminary experiments

We first carried out x-ray diffraction experiments using a Weissenberg camera to check the lattice constants. As a result, we obtained the same values of $a_p \times b_p \times c_p$ as were reported by Völlenkle *et al*. However, we found new superlattice reflections which had the indices $(h/2\ k\ l/4)_p$ (where $(\quad)_p$ means indices defined in the $(a_p\ b_p\ c_p)$ cell), in addition to the fundamental reflections related to the pseudo-unit cell, $a_p \times b_p \times c_p$. The intensity of the newly found superlattice reflections was extremely weak compared with that of the fundamental ones. We also examined several samples prepared from the as-grown crystals, but it was impossible to detect the superlattice reflections that were found for the annealed and slowly cooled sample.

To obtain more accurate information from the new superlattice reflections, we employed an energy-dispersive x-ray diffraction method [9], in which the energy of the photons was analysed by a multichannel analyser. This method improves on the conventional x-ray diffraction one as regards the measurement of weak reflections for the following reason. Since the energy of photons diffracted from the sample is analysed by a solid-state detector installed in the multichannel analyser, photons arising from any kind of fluorescence are avoided, and, therefore, the background counts are extremely reduced in number. Furthermore, photons diffracted from the same part of the sample are counted under the condition that the Bragg angle between the sample and the detector is fixed, which enables one to resolve any ambiguity arising from variations in the scattering of the sample thickness from part to part. In the present experiments, we used an Au rotational anode as the source of the white x-ray beam. Details of the instrument have already been reported [9].

Among the several peaks created from the new superlattice structure, figure 2 shows a representative one observed by the energy-dispersive method, i.e., the peak profile of the $(5\ 0\ 3/4)_p$ superlattice reflection, in which the ordinate indicates the number of photons and the abscissa indicates the energy of the diffracted photons. The data were taken by exposing the sample to x-ray beams with a power of about 40 kV × 60 mA for 20 s. If the crystal symmetry is that given by *Pbmm*, the reflection shown in figure 2 never appears. As a result of the preliminary experiments mentioned above, we find that the crystal structure of $CuGeO_3$ has the unit cell $2a_p \times b_p \times 4c_p$, where $a_p \times b_p \times c_p$ indicates the unit cell proposed by Völlenkle *et al*.

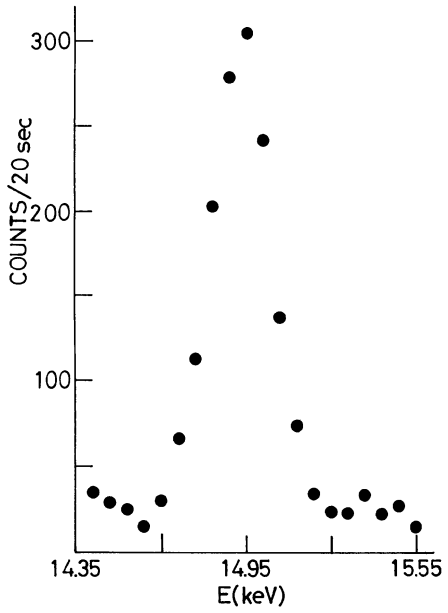

Figure 2. An example of the peak profile of the superlattice reflection indexed as $(5\ 0\ 3/4)_p$, which is newly found at room temperature by an energy-dispersive x-ray diffraction method.

3.2. Structural refinement

To obtain more detailed information about the crystal structure, we performed experiments using a four-circle x-ray diffractometer with a rotating Mo anode as the power source of the 60 kV and 100 mA x-ray, and tried to detect reflections for the Bragg angles below 30.0°. Because the crystals of the present compound have strong cleavability along the a-plane, it was impossible to shape the samples into spheres. As a result, we were obliged to employ a parallelepiped-shaped sample. The size of the sample was about $0.3 \times 0.3 \times 0.1$ mm^3. From this experiment, we were able to observe 950 reflections with the structure factor $F_{obs} \neq 0$. We performed a full-matrix least-squares refinement for 450 independent reflections which had $F_{obs} > 2\sigma$ where σ was the standard deviation, by which the statistical errors were reduced. The convergence factor R was 0.095, where $R = (\sum |F_{obs} - \kappa|F_{cal}||)/\sum |F_{obs}|$, in which κ is the scaling factor. If a spherical sample had been available, the value of R could have been reduced. From the refinement of the observed reflections, we, as a result, determine the lattice parameters to be $a = 9.5998$ Å, $b = 8.4665$ Å and $c = 11.778$ Å, while the space group is found to be $P2_12_12$ (D_2^3). The unit cell, $a \times b \times c$, corresponds to $2a_p \times b_p \times 4c_p$, and therefore the number of quasi-molecules $CuGeO_3$ in the unit cell is 16. The newly found reflections have a systematic rule, i.e., the reflections which should be indexed as (h 0 0) and (0 k 0) with $h, k =$ odd are completely absent, where ( ) indicates the indices defined in the (a b c) cell.

The final values of the structural parameters are given in tables 1 and 2 in which the standard deviations are given in parentheses. The parameters that indicate the positions of the Cu ions given in table 1 are simple, whereas those of the Ge ions are suggestive. That is, the X-coordinates of Ge 1–Ge 4 which successively align along the c-axis are slightly different from one another, which was not found in the study [6]. To be more precise, their

Table 1. Structural parameters for Cu and Ge ions determined at room temperature. The standard deviations are given in parentheses. B_{11}, B_{22} and B_{33} are the anisotropic temperature factors. Cu 1–Cu 4 are surrounded by the O ions labelled $03j$ and $01j$, while Cu 5–Cu 8 are surrounded by those labelled $02j$ and $01j$ ($j = 1$–4), where the positions of the O ions are given in table 2.

Atom	X	Y	Z	B_{11}	B_{22}	B_{33}
Cu 1	0.00	0.00	0.00	0.0147(22)	0.0016(11)	0.0127(15)
Cu 2	0.00	0.00	0.25	0.0152(16)	0.0011(9)	0.0003(3)
Cu 3	0.00	0.00	0.50	0.0082(11)	0.0003(7)	0.0006(3)
Cu 4	0.00	0.00	0.75	0.0278(37)	0.0063(16)	0.0010(3)
Cu 5	0.00	0.50	0.00	0.0013(5)	0.0016(7)	0.0010(3)
Cu 6	0.00	0.50	0.25	0.0100(17)	0.0009(8)	0.0009(4)
Cu 7	0.00	0.50	0.50	0.0013(7)	0.0073(12)	0.0046(6)
Cu 8	0.00	0.50	0.75	0.0184(22)	0.0102(17)	0.0008(4)
Ge 1	0.2932(7)	0.25	0.125	0.0169(10)	0.0058(6)	0.0013(3)
Ge 2	0.2879(3)	0.25	0.375	0.0005(3)	0.0015(4)	0.0071(4)
Ge 3	0.2822(6)	0.25	0.625	0.0097(5)	0.0008(4)	0.0024(3)
Ge 4	0.2852(5)	0.25	0.875	0.0086(5)	0.0037(5)	0.0013(2)

Table 2. Structural parameters for the O ions labelled $01j$, $02j$ and $03j$ with $j = 1$–4 determined at room temperature. B_{00} is the isotropic temperature factor and the standard deviations are given in parentheses.

O atom	X	Y	Z	B_0
011	0.1793(31)	0.2388(51)	0.00	1.33(46)
012	0.2065(39)	0.2299(51)	0.25	1.92(60)
013	0.1774(29)	0.2373(49)	0.50	1.11(42)
014	0.1957(34)	0.2517(63)	0.75	1.78(47)
021	0.3971(39)	0.0963(38)	0.125	1.03(45)
022	0.4199(39)	0.0882(40)	0.375	1.45(51)
023	0.3970(24)	0.0838(36)	0.625	0.86(43)
024	0.3776(4)	0.0652(46)	0.875	1.87(59)
031	0.3840(33)	0.4303(38)	0.125	0.87(45)
032	0.3446(45)	0.4334(47)	0.375	2.22(64)
033	0.3915(33)	0.4159(37)	0.625	0.95(44)
034	0.4053(38)	0.4167(40)	0.875	1.34(49)

X-coordinates change periodically with the period $4c_p$. As will be shown later, this change is closely related to the tilting of the GeO_4 tetrahedra from a line parallel to the c-axis.

To show an outline of the newly determined unit cell, we draw the Z-projection of the arrangement of the Cu, Ge and O ions in figure 3, in which the Cu and O ions with $Z = 1/4$ as well as the O and Ge ions with $Z = 3/8$ are projected on the $Z = 1/4$ level. The notation 01, 02 and 03 used in figure 3 indicates the O ions labelled in table 2 as 012, 022 and 032, respectively; 012 is located on the $Z = 1/4$ level, while 022 and 032 are on the $Z = 3/8$ level. The Ge ions shown in figure 3 are those on the $Z = 3/8$ level. As can be seen in figure 3, the GeO_4 tetrahedra are slightly rotated around the lines parallel to the c-axis (the Z-axis) with the directions of rotation of the adjacent tetrahedra in the ab-plane in anti-phase to one another, as indicated by curved arrows. As a result

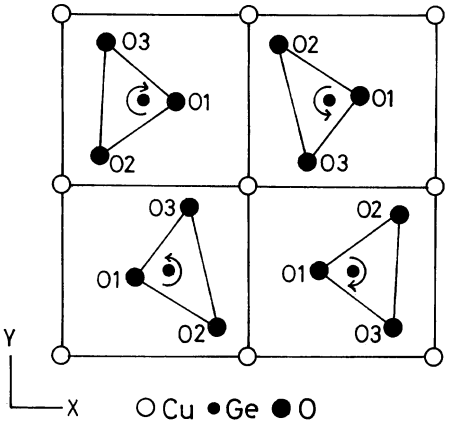

Figure 3. The newly found structure projected on the $Z = 1/4$ and $3/8$ levels. The labels 01, 02 and 03 attached to the O ions are abbreviations of 012, 022 and 032 given in table 2; 01 ions are on the $Z = 1/4$ level, while 02 and 03 ions are on the $Z = 3/8$ level. The Cu and Ge ions are those on the $Z = 1/4$ and $3/8$ levels, respectively. The curved arrows indicate the directions of the rotations of the GeO_4 tetrahedra.

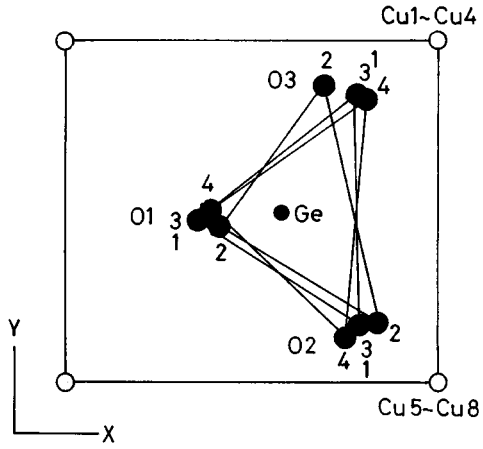

Figure 4. A quarter of figure 3, i.e., a quarter of $2a_p \times b_p$. The rotation scheme of the GeO_4 tetrahedra in the unit cell, $a \times b \times c$, is projected on a Z-level. The labels 01, 02 and 03 attached to the O ions are abbreviations of 012, 022 and 032 which are given in table 2, and the numbers 1, 2, 3 and 4 indicate the labels j of the O ions $01j$, $02j$ and $03j$ ($j = 1$–4) which are also defined in table 2. The projected sites of the O ions denoted as $j = 1$ and 3 almost overlap each other for all of the $01j$, $02j$ and $03j$ series.

of the rotation, the site of the O ions denoted as 02 in figure 1(b) divides into two kinds of site, 02 and 03, which are different from each other. Figure 4 shows a quarter of the Z-projection shown in figure 3; the Z-projections of the series of the four GeO_4 tetrahedra aligned along the c-axis are presented. The notation 01, 02 and 03 given in figure 4 has the same meaning as that in figure 3 used to classify the O ions. The numbers 1, 2, 3 and 4 attached to the O ions in figure 4 indicate the values of j in $01j$, $02j$ and $03j$ ($j = 1$–4) which are given in table 2. The O ions labelled as 011, 012, 013 and 014 in table 2 have

the Z-components $Z = 0, 1/4, 2/4$ and $3/4$, respectively, while those labelled 021 and 031 have $Z = 1/8$, those labelled 022 and 032 have $Z = 3/8$, those labelled 023 and 033 have $Z = 5/8$, and those labelled 024 and 034 have $Z = 7/8$. The respective four Ge ions with $Z = 1/8, 3/8, 5/8$ and $7/8$ are shown at the same XY-coordinates to simplify the figure, i.e., the minute differences among the X-coordinates of Ge 1–Ge 4 shown in table 1 are temporarily ignored.

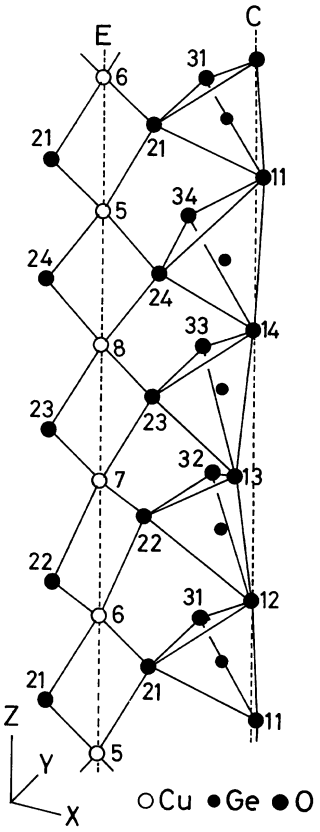

Figure 5. A schematic drawing of the quasi-one-dimensional stacking of the CuO_6 octahedra along the straight line E, and the one-dimensional zigzag linkage of the edges of the GeO_4 tetrahedra along another straight line C. Both lines, C and E, are parallel to the c-axis.

From figures 3 and 4, we find that the four GeO_4 tetrahedra stacked along the c-axis are almost identical in shape, but they are tilted differently from one another from a straight line denoted as C in figure 2 and figure 5 which will be explained below, and they are also differently rotated around a line parallel to the c-axis. The series of GeO_4 tetrahedra stacked along the c-axis in the remaining three quarters of figure 3 also have tiltings and rotations which are similar to those shown in figure 4. As a result, we find that a periodic change of the tilting and the rotation is formed along the c-axis with the period of $4c_p$. The different manners of the tiltings accompany the shifts of the positions of the Ge ions enclosed in the tetrahedra; the shift appears as a change of the coordinate X, as shown in table 1 and explained earlier in this section. Moreover, we find in figure 3 that the manners of tilting and rotation of the adjacent GeO_4 tetrahedra along the a-axis are different from each

other, i.e., the directions of their rotations are in anti-phase, as indicated by curved arrows. This fact results in a doubling of the pseudo-unit cell $a_p \times b_p \times c_p$ along the a-axis. The experiments reported in [6] also failed to detect the tilting and the rotation mentioned above, i.e., their results suggest that one of the edges of the respective GeO_4 tetrahedra which are identical as regards their shapes aligns straight along the line C without accompanying the rotations, as shown in figure 1(b).

The four-times periodicity, i.e., the $4c_p$-periodicity, of the superlattice structure along the c-axis is closely related to the regularity of the tilting and the rotation schemes of the GeO_4 tetrahedra, as explained above. Due to the tilting and the rotation of the surrounding GeO_4 tetrahedra, each CuO_6 octahedron is fairly distorted because the CuO_6 octahedra and the GeO_4 tetrahedra share the O ions, as shown in figures 1 and 3. On the basis of figure 4, we schematically draw in figure 5 the arrangement of the GeO_4 tetrahedra and the CuO_6 octahedra stacked along the c-axis, in which the numbers $i = 5$–8 indicate the Cu ions, and the 11, 12, 21, 22, 31, 32, ... attached to the O ions are abbreviations of 011, 012, 021, 022, 031, 032, ... which are given in table 2. We find in figure 5 a zigzag alignment on one of the edges of the GeO_4 tetrahedra. The Cu chain drawn in figure 5 consists of the bondings through O($02j$) ions. A similar Cu chain, i.e., a cyclic arrangement of the Cu 1–Cu 4, is also formed with the bondings through O($03j$) ions. Thus the two kinds of Cu chain along the c-axis must be considered.

We now compare the environment of the Cu ions in the old structure given in [6] with that in the newly determined structure. In the old structure shown in figures 1(a) and 1(b), the O(02) ions aligned on the A and B lines look like they form a ladder. The two side-pieces (legs) of the ladder, i.e., the linkages of the O(02) ions along the A and B lines, are parallel to each other, and the rungs of the ladder, i.e., the O(02)–O(02) bonding lines in the ab-plane, are also parallel to one another. In the newly determined structure, in contrast, the two side-pieces (legs) form zigzag lines, and the adjacent rungs, i.e., the O($02j$)–O($02j$) or O($03j$)–O($03j$) bonding lines, are not parallel any more; in both in cases this is due to the tiltings and rotations of the GeO_4 tetrahedra which share the O ions with the CuO_6 octahedra. As a whole, the ladder seems to be twisted around the Cu–Cu line, i.e., the line E which is shown in figure 5, and the twist has a periodicity of $4c_p$.

From these facts, we point out that the four CuO_6 octahedra which are distorted differently from one another are stacked regularly along line E, which is parallel to the c-axis, as shown in figure 5. Such distortions are induced by the displacement of O ions, 02 ($02j$) and 03 ($03j$), caused by the tilting and the rotation of the GeO_4 tetrahedra. The fact that the new superlattice reflections were detected indicates a coherent alignment of the differently distorted CuO_6 octahedra (and differently tilted and rotated GeO_4 tetrahedra) in the sample. The samples which lack such a coherency probably yield results similar to the one reported in [6].

Using the refined structural parameters for Cu, Ge and O ions which are given in tables 1 and 2, we determine the lengths of the bonds between Ge and O ions in the GeO_4 tetrahedra as well as those between Cu and O ions in the CuO_6 octahedra. The notation k, l, m and n is used to define the bond lengths, as shown in figure 6. We list their values in tables 3 and 4. Furthermore, the distances between the two O ions, i.e., $02j$ and $02j$, or $03j$ and $03j$, which are shared with the adjacent CuO_6 octahedra along the c-axis, are also listed in table 4 as d_1 and d_2, both of which are found to change periodically. The mean values of the respective bond lengths are also shown in tables 3 and 4 for comparison with those given in [6]. As the final data obtained in the present experiments, we show the Cui–O($02j$)–Cui' ($i, i' = 5$–8) and Cui–O($03j$)–Cui' ($i, i' = 1$–4) bond angles in table 5 together with their mean value and that given in [6]. These angles, as well as the bond lengths k, l and

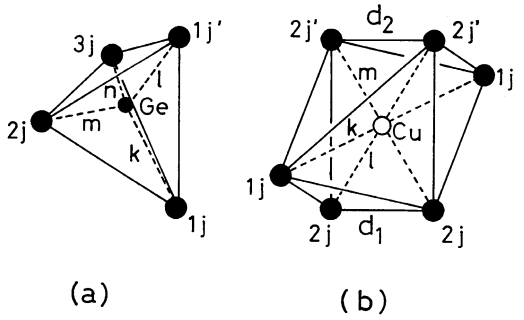

Figure 6. Bond lengths in (a) the GeO_4 tetrahedron and (b) the CuO_6 octahedron. d_1 and d_2 in (b) indicate the distances between the two O ions which are shared with the adjacent CuO_6 octahedra along the c-axis. The lengths k, l, m and n in (a) and k, l and m in (b) are given in tables 3 and 4, respectively. The labels $1j$, $1j'$, $2j$, $2j'$ and $3j$ attached to the O ions are abbreviations of $01j, 01j', 02j, 02j'$ and $03j$, respectively, and j and j' cycle through the numbers 1–4. (b) shows the CuO_6 octahedron which consists of O($01j$) and O($02j$). The same definition of k, l and m also applies to the octahedron formed by O($01j$) and O($03j$).

Table 3. Shape parameters for each GeO_4 tetrahedron determined at room temperature. k, l, m and n are the lengths of the bonds among the Ge ion and the O ions which surround the Ge ion, as indicated in figure 6(a). Ge 1–Ge 4 correspond to those shown in figure 6(a). The standard deviations are given in parentheses. Their mean values and the lengths given in [6] are also shown for comparison.

Atom	k (Å)	l (Å)	m (Å)	n (Å)
Ge 1	1.836(48)	1.699(44)	1.641(34)	1.758(32)
Ge 2	1.675(43)	1.817(42)	1.867(37)	1.646(43)
Ge 3	1.786(42)	1.690(53)	1.787(33)	1.754(32)
Ge 4	1.704(53)	1.791(41)	1.799(40)	1.823(37)
Mean value	$(\sum k + \sum l)/8 = 1.750(46)$		$(\sum m + \sum n)/8 = 1.759(36)$	
Value given in [6]	1.769		1.724	

m within the CuO_6 octahedra, are important in discussing the superexchange interactions between the nearest-neighbour Cu spins on the c-axis.

The data shown and explained above show the different manners of distortion of the GeO_4 tetrahedra and the CuO_6 octahedra. Furthermore, the shapes of the CuO_6 octahedra seem to be triclinic—in contrast to the ligand octahedra in various copper halide compounds in which the ligand octahedra are distorted to tetragonal or orthorhombic shapes due to the Jahn–Teller effect. The ratio of the shortest axis to the longest one, i.e., l/k or m/k, for the CuO_6 octahedra is fairly large compared with that of the ligand octahedra in the copper halide compounds. We therefore think that the distortion of the CuO_6 octahedra in $CuGeO_3$ is not caused by the Jahn–Teller effect. Rather, the shapes of the CuO_6 octahedra are governed by the surrounding GeO_4 tetrahedra.

4. Discussion

As developed in section 3, the present experiments have made it clear that GeO_4 tetrahedra are tilted and rotated in four different manners at room temperature. The linkage of one

Table 4. Shape parameters for each of the CuO_6 octahedra determined at room temperature. The standard deviations are given in parentheses. As shown in figure 6(b), k, l and m are the distances apart of the Cu ion and the O ions which surround the Cu ion, while d_1 and d_2 are those of the two O ions which are shared with adjacent CuO_6 octahedra stacked along the c-axis. Cu 1–Cu 4 are surrounded by the O ions labelled $03j$ and $01j$, while Cu 5–Cu 8 are surrounded by ones labelled $02j$ and $01j$. From the definition of d_1 and d_2 and the four-times periodicity, the values of d_1 for Cu 2, Cu 3 and Cu 4 correspond to the values of d_2 for Cu 1, Cu 2 and Cu 3, respectively, and d_1 for Cu 1 is the same as d_2 for Cu 4. The same can be said for Cu 5–Cu 8. The mean values and the bond lengths determined in [6] are also shown.

Atom	k (Å)	l (Å)	m (Å)	d_1 (Å)	d_2 (Å)
Cu 1	2.656(47)	1.884(35)	1.943(30)	2.302	2.521
Cu 2	2.778(43)	1.943(30)	2.153(41)	2.521	3.190
Cu 3	2.634(42)	2.153(41)	1.930(32)	3.190	2.524
Cu 4	2.842(53)	1.930(32)	1.884(35)	2.524	2.302
Cu 5	2.803(44)	1.952(40)	1.959(32)	2.597	2.562
Cu 6	3.027(43)	1.959(32)	1.816(36)	2.562	2.144
Cu 7	2.802(42)	1.816(36)	1.905(32)	2.144	2.598
Cu 8	2.820(53)	1.905(32)	1.952(40)	2.598	2.597
Mean value	2.795(46)	1.943(35)	1.943(35)	2.555	2.555
Value given in [6]	2.766	1.942		2.538	

Table 5. Bond angles which are relevant to the superexchange interactions between the nearest-neighbour Cu spins on the c-axis through $O(02j)$ and $O(03j)$ ($j = 1$–4). The two angles which are formed by the two Cui–$O(02j)$–Cui' paths (or the two Cui–$O(03j)$–Cui' paths) and are facing each other are identical. The numbers in parentheses are the standard deviations. The mean value and the angle determined in [6] are also shown.

Bond	Angle (deg)	Bond	Angle (deg)
Cu 1–O(031)–Cu 2	98.4(1.3)	Cu 5–O(021)–Cu 6	97.4(1.4)
Cu 2–O(032)–Cu 3	86.2(1.5)	Cu 6–O(022)–Cu 7	108.2(1.9)
Cu 3–O(033)–Cu 4	99.3(1.5)	Cu 7–O(023)–Cu 8	101.1(1.5)
Cu 4–O(034)–Cu 1	102.7(1.7)	Cu 8–O(024)–Cu 5	97.8(1.7)
Mean value of the eight angles given above		98.89(1.6)	
Value given in [6]		98.41	

of the edges of the tilted GeO_4 tetrahedra forms a four-times periodic zigzag chain along the c-axis, as shown in figure 5, and the rotation of the tetrahedra also has a four-times periodicity along the c-axis. Such tiltings and rotations of the GeO_4 tetrahedra induce local distortions of the CuO_6 octahedra with the four-times periodicity along the c-axis.

Looking at the mean values of the bond lengths and the bond angles which are given in tables 3, 4 and 5, we find that they coincide with the bond lengths and the bond angle given in [6] within experimental errors. This fact strongly indicates that the crystal structure reported in [6] merely presents an averaged shape of the differently distorted octahedra (tetrahedra), which is due to the lack of coherency of the distortions in the samples used in [6], as we have suggested in section 1.

Because of such a periodicity of the structure along the c-axis, the midpoint between the nearest-neighbour Cu sites on the c-axis is not an inversion centre any more, which indicates the existence of the DM interaction in the present compound—which was revealed in the

EPR investigation [7]. Since DM interaction depends on the local symmetry around the nearest-neighbour spins on the c-axis, it does not matter whether the coherency of the distortions is created in the sample or not. In other words, the as-grown crystals and the annealed ones yield identical EPR spectra.

The structural parameters given in tables 4 and 5, i.e., k, l and m for the CuO_6 octahedra and bond angles, indicate that neither the superexchange interactions between the nearest-neighbour Cu spins on the c-axis through the O($02j$) ions nor those through the O($03j$) ions are unique, because the respective bond lengths relevant to the superexchange interactions, i.e., l and m for Cu 1–Cu 4 (or Cu 5–Cu 8), are different from one another and the bond angles are not identical. From these facts, we conclude, in spite of the regular intervals between the Cu ions on the c-axis for $T > T_{sp}$, that the superexchange interactions between the nearest-neighbour Cu spins along the c-axis have four different values, although the differences among them are expected to be very small. Moreover, the four respective superexchange interactions through the O($03j$) ions do not necessarily coincide with those through O($02j$), as the bond angles and the bond lengths, l and m, for Cu 1–Cu 4 and Cu 5–Cu 8 suggest. We must thus consider two kinds of magnetic chain along the c-axis, which have four different superexchange interactions individually.

As a result of the different manners of distortion which appeared in the CuO_6 octahedra, the Cu–O and O–O interionic potentials of the respective CuO_6 octahedra are slightly different from one another. The differences are expected to be so small as to be easily overcome by thermal fluctuations of the lattice at high temperatures. In other words, the order of the distortions is easily destroyed by thermal fluctuations at high temperatures. This is why the as-grown crystals obtained by the FZ method have neither the coherency of distortions of the CuO_6 octahedra nor that of the tilting and the rotation of the GeO_4 tetrahedra. That is, a fast cooling of the melt in the FZ method freezes the thermal fluctuation of O ions before they occupy their respective proper stable sites, as if the samples were quenched.

At a certain low temperature, the antiferromagnetic energy of coupling between the Cu spins on the c-axis will overcome the differences of the interionic potentials mentioned above, and it will force the O ions to slightly change their positions, which can be a source of the dimerization of the Cu ions confirmed to occur in this inorganic compound.

We now discuss a relationship between the room temperature structure discovered in the present study and that expected below T_{sp}. The dimerization of the Cu^{2+} spins along the c-axis leads to a superlattice structure different from that observed above T_{sp}. Actually, electron diffraction experiments [4] revealed new superlattice reflections with indices $(h/2\ k\ l/2)_p$ (h, k, l all odd), while neutron diffraction measurements [2] also found additional reflections with $k =$ even. These results indicate that the unit cell of the structure below T_{sp} can be expressed as $2a_p \times b_p \times 2c_p$. The unit cell thus changes from $2a_p \times b_p \times 4c_p$ to $2a_p \times b_p \times 2c_p$ when the temperature is decreased across T_{sp}. The appearance of the two-times periodicity, i.e., the $2c_p$-periodicity, along the c-axis suggests that an anti-phase rotation and tilting of the adjacent GeO_4 tetrahedra arranged along the c-axis is induced below T_{sp}.

Figures 7(a) and 7(b) schematically show the structures expected below T_{sp}; two possible models of the arrangements of ions projected on the Z-plane are shown in the respective figures, in which the solid and dotted lines indicate the adjacent GeO_4 tetrahedra and CuO_6 octahedra individually stacked along the c-axis. The difference between figure 7(a) and figure 7(b) lies in whether the bonding lines connecting O ions, i.e., $01j$ with $j =$ 1–4, are on a straight line parallel to the c-axis or not. In other words, the GeO_4 tetrahedra shown in figure 7(a) have both the rotations and tiltings, whereas those shown in figure 7(b)

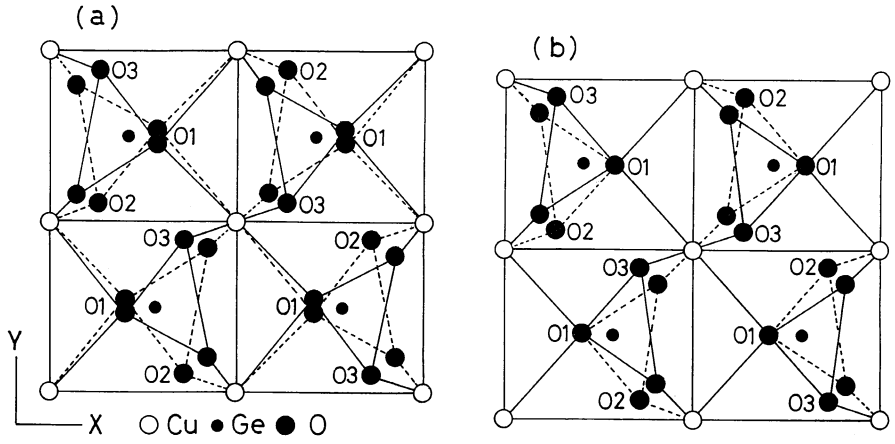

Figure 7. The Z-projection of models of the structure expected below T_{sp}. The bonding lines among the O ions labelled as $01j$ (j = 1–4) form a zigzag line in (a), which is due to the rotation and tilting of the GeO_4 tetrahedra, while they form a straight line in (b) because of the absence of tilting of the GeO_4 tetrahedra.

have only the rotations. We find in these two figures that the directions of rotation of the nearest-neighbour GeO_4 tetrahedra stacked along the c-axis are in anti-phase, which brings about an alternative distortion of the CuO_6 octahedron along the c-axis.

On the basis of figure 7(b), we show in figure 8 the arrangements of both the CuO_6 and GeO_4 polyhedra along the c-axis, in which one finds that the O ions denoted as 11 and 12 (abbreviations of 011 and 012, respectively) are on the straight line C which is parallel to the c-axis. These models of the structure expected below T_{sp} still show a difference between the lengths of bonds of the two O ions, i.e., $02j$ and $02j$, or $03j$ and $03j$, which are shared with the nearest-neighbouring CuO_6 octahedra stacked along the c-axis. The anti-phase rotation of the GeO_4 tetrahedra around the c-axis will induce an alternative difference of the O($02j$)–O($02j$) (and O($03j$)–O($03j$)) bond lengths. That is, the four-times periodic change of d_1 and d_2 shown in table 4 will be reduced to the two-times one. As a result, the Cu ions will be dimerized along the c-axis, as indicated in figure 8.

The discussion for the structural transition at T_{sp} given above is based on the model where the periodicity along the c-axis directly changes from $4c_p$ to $2c_p$. However, other models are not ruled out. The degree of the rotation and tilting of the GeO_4 tetrahedra will change with temperature. With temperature decreasing toward T_{sp}, the four-times periodic order of the distortions will be disturbed and will become unstable, and then it would be possible for a virtual order of the distortions to arise with, for instance, three-times periodicity ($3c_p$), and incommensurate arrangements of the distortions could appear above T_{sp}. Such instability induces the fluctuations of the superexchange interactions which have four different values at room temperature. This fact, we believe, affects magnetic properties over the short-range-ordering region. As was pointed out earlier [1], the susceptibility does not fit the Bonner–Fisher curve over the magnetic short-range-ordering region. But what if we try to explain this contradiction by taking into account the fluctuations of the superexchange interactions which have four different values at room temperature? On the other hand, the diffraction and optical experiments so far performed could not find the phonon mode which is expected to freeze at T_{sp}. We point out that as-grown crystals were used in those experiments—crystals which, we believe, lacked the coherency of the

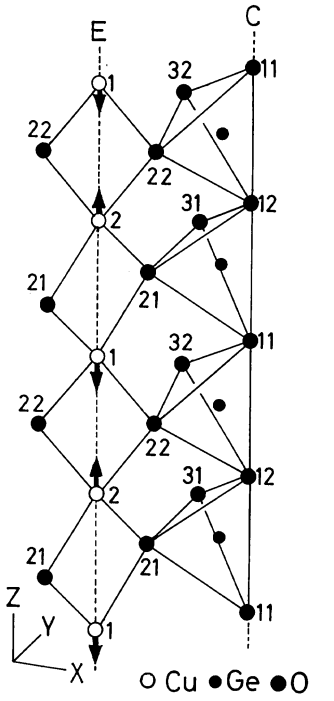

Figure 8. A model of the dimerized structure. The arrows indicate the directions of the displacement of Cu ions due to dimerization.

distortions of the polyhedra. The phonon mode which is created from the coherency of the distortions formed along the *c*-axis is expected to freeze at T_{sp}. Accordingly, it is a matter of course that the phonon freezing, if it really exists, cannot be observed as long as one uses as-grown crystals obtained by the FZ method.

Thus far in this and previous sections, we have only considered the one-dimensional aspect of the stacking of two kinds of polyhedron. However, we should point out that a two-dimensional character is induced when the coherency of the tiltings and the rotations of the GeO_4 tetrahedra along the *c*-axis is completely destroyed. The complete absence of coherency along the *c*-axis indicates that the adjacent GeO_4 tetrahedra on the *c*-axis have no correlations in their manners of tilting and rotation, and consequently networks of the tiltings and rotations of the tetrahedra spread two dimensionally in the *ab*-plane. As is well known, samples which lack such coherency along the *c*-axis have the possibility of showing rod-type diffuse reflections along the c^*-axis. For this reason, the rod-like diffuse streaks observed along the c^*-direction in electron diffraction experiments [4] performed on the as-grown sample need to be re-examined using well annealed samples. We believe that such rod-type diffuse reflections are excluded in well annealed samples.

For reference, we point out that the rod-type reflections reported in [4] probably correspond to those observed in the diluted Jahn–Teller system $K_2Cu_xZn_{1-x}F_4$ with $x = 0.8$ [10]. That is, the correlations of the distortions of the CuF_6 octahedra along the *c*-axis in K_2CuF_4 ($x = 1$) are destroyed by the random replacement of Cu ions with Zn ions, and then rod-type reflections are yielded instead of the spot-like reflections which are observed for K_2CuF_4 and seen as evidence of the three-dimensional correlations of the Jahn–Teller distortions of CuF_6 octahedra.

The ribbon-like diffuse scattering observed parallel to the c^*-axis which was reported in another electron diffraction study [11] must be also re-examined for samples which have

coherent distortions, because we cannot silence a fear that the lack of coherency brings about this kind of ribbon-like scattering.

5. Conclusion

From the present room temperature x-ray diffraction experiments performed on carefully prepared samples of $CuGeO_3$, we have shown the crystal symmetry with space group *Pbmm* reported by Völlenkle *et al* to be incorrect. On the basis of the newly detected superlattice reflections, the space group and the lattice parameters have been found to be $P2_12_12$ and $2a_p \times b_p \times 4c_p$, respectively, where $a_p \times b_p \times c_p$ is the pseudo-unit cell proposed by Völlenkle *et al*. Since in the four-times periodic structure along the *c*-axis it is not possible for the midpoint between the nearest-neighbour Cu sites on the *c*-axis to be an inversion centre, DM interaction is allowed, the existence of which is revealed by EPR study. We have also found two kinds of magnetic chain along the *c*-axis, which have four different superexchange interactions individually.

One of the key points which led to the success in detecting the new superlattice reflections is the improved quality of the samples achieved by the annealing and slow cooling of the as-grown crystals obtained by the floating-zone method. The experiments performed on the as-grown single crystals were unable to reveal the superlattice structure, probably because the coherency of distortions was destroyed during the fast crystallization process. The crystal structure proposed by Völlenkle *et al* has been found to merely reflect an averaged shape of the eight differently distorted CuO_6 octahedra (and four differently tilted and rotated GeO_4 tetrahedra) because of the poor quality of the sample. By annealing and slowly cooling the as-grown crystals, the coherency of the manners of distortion is regained. Before concluding the present report, we emphasize that various investigations performed on the as-grown single crystals obtained by the floating-zone method must be critically re-examined. Our neutron diffraction experiments over the lower-temperature region are now in progress.

Acknowledgments

We acknowledge Mr O Fujita for growing the crystals by the floating-zone method. One of the authors (IY) is grateful to Professors K Motizuki and K Uchinokura for their interest in our study and several valuable comments.

References

[1] Hase M, Terasaki L and Uchinokura K 1993 *Phys. Rev. Lett.* **70** 3651
[2] Hirota K, Cox D E, Lorenzo J E, Shirane G, Tranquada J M, Hase M, Uchinokura K, Kojima H, Shibuya Y and Takano 1994 *Phys. Rev. Lett.* **73** 736
[3] Pouget J P, Regnault L P, Ain M, Hennion B, Renard J P, Veillet P, Dhalenne G and Revcolevschi A 1994 *Phys. Rev. Lett.* **72** 4037
[4] Kamimura O, Terauchi M, Tanaka M, Fujita O and Akimitsu J 1994 *J. Phys. Soc Japan* **63** 2467
[5] Nishi M, Fujita O and Akimitsu J 1994 *Phys. Rev.* B **50** 6508
[6] Völlenkle H, Wittmann A and Nowotny H 1967 *Monatsh. Chem.* **98** 1352
[7] Yamada I, Nishi M and Akimitsu J 1996 *J. Phys.: Condens. Matter* **8** 2625
[8] Moriya T 1960 *Phys. Rev.* **120** 91
[9] Hidaka M, Akiyama H and Wanklyn B M 1986 *Phys. Status Solidi* b **97** 387 and the references therein
[10] Hidaka M, Inoue K, Yamada I and Walker P J 1983 *Physica* B **121** 343
[11] Chen C H and Cheong S-W 1995 *Phys. Rev.* B **51** 6777